Incomplete lineage sorting and speciation without morphological change in ghost-worm cryptic species

José Cerca [Corresp., 1, 2, 3], **Angel Rivera-Colon** [4], **Mafalda Ferreira** [5, 6, 7], **Mark Ravinet** [8, 9], **Michael Nowak** [3], **Julian Catchen** [4], **Torsten Struck** [3]

[1] Department of Environmental Science, Policy, and Management, University of California, University of California, Berkeley, Berkeley, California, United States

[2] Department of Natural History, NTNU University Museum, Norwegian University of Science and Technology, Trondheim, Norway

[3] Natural History Museum, University of Oslo, Oslo, Norway

[4] Department of Evolution, Ecology, and Behavior, University of Illinois at Urbana-Champaign, Urbana Champaign, Illinois, United States

[5] Division of Biological Sciences, University of Montana, Missoula, Montana, United States

[6] Departamento de Biologia, Universidade do Porto, Porto, Porto, Portugal

[7] CIBIO, Centro de Investigação em Biodiversidade e Recursos Genéticos, InBIO Laboratório Associado, Universidade do Porto, Porto, Porto, Portugal

[8] School of Life Sciences, University of Nottingham, Nottingham, United Kingdom

[9] Centre for Ecological and Evolutionary Synthesis, University of Oslo, Oslo, Norway

Corresponding Author: José Cerca
Email address: jose.cerca@ntnu.no

Morphologically similar species, that is cryptic species, may be similar or quasi-similar owing to the deceleration of morphological evolution and stasis. While the factors underlying the deceleration of morphological evolution or stasis in cryptic species remain unknown, decades of research in paleontology on punctuated equilibrium have originated clear hypotheses. Species are expected to remain morphologically identical in scenarios of shared genetic variation, such as hybridization and incomplete lineage sorting, or in scenarios where bottlenecks reduce genetic variation and constrain the evolution of morphology. Here, focusing on three morphologically similar *Stygocapitella* species, we employ a whole-genome amplification method (WGA) coupled with double-digestion restriction-site associated DNA sequencing (ddRAD) to reconstruct the evolutionary history of the species complex. We explore population structure, use population-level statistics to determine the degree of connectivity between populations and species, and determine the most likely demographic scenarios which exclude evidence for recent hybridization. We find that the combination of WGA and ddRAD allowed us to obtain genomic-level data from microscopic eukaryotes (~1 millimetre) opening up opportunities for those working with population genomics and phylogenomics in such taxa. The three species share genetic variance, likely from incomplete lineage sorting. We speculate that the degree of shared variation might underlie morphological similarity in the Atlantic species complex.

Incomplete lineage sorting and speciation without morphological change in ghost-worm cryptic species

José Cerca[1,2,3], Angel Rivera-Colón[4], Mafalda S. Ferreira[5,6,7], Mark Ravinet[8,9], Michael D. Nowak[1], Julian Catchen[4], Torsten H. Struck[1]

[1] Natural History Museum, University of Oslo, Oslo, Norway
[2] Department of Environmental Science, Policy, and Management, University of California, Berkeley, CA, USA
[3] Department of Natural History, NTNU University Museum, Norwegian University of Science and Technology, Trondheim, Norway
[4] Department of Evolution, Ecology, and Behavior, University of Illinois at Urbana-Champaign
[5] CIBIO, Centro de Investigação em Biodiversidade e Recursos Genéticos, InBIO Laboratório Associado, Universidade do Porto, Vairão, Portugal
[6] Departamento de Biologia, Faculdade de Ciências da Universidade do Porto, Porto, Portugal
[7] Division of Biological Sciences, University of Montana, Missoula, Montana, USA
[8] Centre for Ecological and Evolutionary Synthesis, University of Oslo
[9] School of Life Sciences, University of Nottingham, UK

Corresponding Author:
José Cerca[1]
ORCID 0000-0001-7788-4367
Sars' Gate 1, Oslo, Norway
Email address: jose.cerca@ntnu.no

Abstract

Morphologically similar species, that is cryptic species, may be similar or quasi-similar owing to the deceleration of morphological evolution and stasis. While the factors underlying the deceleration of morphological evolution or stasis in cryptic species remain unknown, decades of research in paleontology on punctuated equilibrium have originated clear hypotheses. Species are expected to remain morphologically identical in scenarios of shared genetic variation, such as hybridization and incomplete lineage sorting, or in scenarios where bottlenecks reduce genetic variation and constrain the evolution of morphology. Here, focusing on three morphologically similar *Stygocapitella* species, we employ a whole-genome amplification method (WGA) coupled with double-digestion restriction-site associated DNA sequencing (ddRAD) to reconstruct the evolutionary history of the species complex. We explore population structure, use population-level statistics to determine the degree of connectivity between populations and species, and determine the most likely demographic scenarios which exclude evidence for recent hybridization. We find that the combination of WGA and ddRAD allowed us to obtain genomic-

level data from microscopic eukaryotes (~1 millimetre) opening up opportunities for those working with population genomics and phylogenomics in such taxa. The three species share genetic variance, likely from incomplete lineage sorting. We speculate that the degree of shared variation might underlie morphological similarity in the Atlantic species complex.

Introduction

The characterization and delimitation of species and populations using DNA sequencing and barcoding has led to the discovery of 'hidden species diversity' in previously established species (Knowlton 1993; Bickford et al. 2007; Pfenninger and Schwenk 2007; Struck et al. 2018). The initial interest in this hidden diversity, that is cryptic species, fuelled a debate on whether these lineages resulted from biases of a morphologically oriented classification of biodiversity or whether they could result from underlying biological phenomena. On one side, proponents of the "artefact model" suggest that populations and species naturally accumulate morphological differences, and it is only the limitations associated with scientific methods that impede the discovery of those differences (Korshunova et al. 2017). On the one other side, the "evolutionary framework" suggests that the deceleration of morphological evolution is a plausible expectation, given the observation of stasis, niche conservatism and constraints in nature. While some of this diversity is potentially attributed to taxonomic artefacts (Korshunova et al. 2017) morphologically similar species – 'true' cryptic species – have been discovered in various branches of the tree of life, thus representing an important part of biodiversity (Pfenninger and Schwenk 2007; Pérez-Ponce de León and Poulin 2016; Cerca et al. 2018; Fišer et al. 2018).

Following centuries of morphologically oriented taxonomy, the existence of "true" cryptic species entails a challenge to the delimitation, discovery and classification of species (Bickford et al. 2007; Fišer et al. 2018; Struck et al. 2018). In the case of morphologically similar species, species delimitation relying on morphology alone will fail to capture the existing species diversity (Pante et al. 2015; Fišer et al. 2018; Chenuil et al. 2019; Struck and Cerca 2019), resulting in the lumping of different species into a single species complex. While much has been written on the consequences of cryptic species in terms of biological systematics, we have only recently begun to understand the impact of cryptic species in other fields of biology. When species are poorly delimited, determination of biogeographic breaks (Weber et al. 2019; Cerca et al. 2020a), inferences on the evolutionary history (Wada et al. 2013; Swift et al. 2016; Struck et al. 2018;

Dufresnes et al. 2019), and the determination of ecological richness of an ecosystem (Chenuil et al. 2019) may be severely compromised. Furthermore, these problems extend outside fundamental fields of biology when species complexes are medically-relevant, such as the *Anopheles* cryptic species complex where not every morphologically-similar species is capable of transmitting malaria (Erlank et al. 2018) or in complexes of parasite species (De León and Nadler 2010; Nadler and De Len 2011), but also in cases of conservation management (Bickford et al. 2007; Bernardo 2011).

While the discovery of cryptic species complexes has increased in the last few years, the resulting debate has focused on whether these are taxonomic artefacts or biologically relevant species. Consequently, the causes underlying morphological similarity remain mostly unexplored. Despite this hindrance, an important source of information may come from palaeontology where stasis has been studied for decades (Eldredge and Gould 1972; Gould 2002), and from the subsequent integration of this evidence with neontological data. A particularly insightful contribution is that of Futuyma (2010), which suggests that stasis may result from certain ecological, genetic and developmental scenarios. Genetic scenarios include shared genetic variation, potentially resulting from hybridization or ILS, homogenizing morphological divergence; genetic constraints resulting from epistatic reactions or pleiotropy, or constrains from the lack of genetic variation due to repeated bottlenecks or founder effects; stabilizing selection on morphology (Futuyma 2010). Some of these scenarios including stabilizing selection (Lee and Frost 2002; Novo et al. 2010, 2012; Lavoué et al. 2011; Smith et al. 2011; Santamaria et al. 2016; Zuccarello et al. 2018), bottlenecks and founder effects (Dornburg et al. 2016; Valtueña et al. 2016) have been proposed to explain similarity on cryptic species. However, this remains untested since evidence for morphological similarity comes from interpretation of indirect methods, such as phylogenetic trees.

The *Stygocapitella* genus includes 11 described species with only four morphotypes and no significant quantitative morphological differences between some species (Cerca et al. 2020a, b). Morphologically identical species occur in sympatry and overlap in their distribution along the Northern European, Atlantic American, and Pacific American coastlines. In a previous study, we confirmed that three North Atlantic species - *Stygocapitella westheidei*, *S. subterranea*, and *S. josemariobrancoi* – are morphologically identical (Cerca et al. 2020a), nonetheless, we were not

able to determine the causes underlying morphological similarity with certainty. Preliminary results from selected DNA markers indicated that morphological similarity potentially stems from niche conservatism and tracking, coupled with the fluctuating dynamics of their habitats and/or genetic constraints (Cerca et al. 2020b). Here, using genomic data, we extend these efforts by focusing on the causes linked to genetic variation underlying morphological similarity (see above). Following Futuyma (2010), we hypothesize that 1) bottlenecks and founder effects reduce genetic variation, thus resulting in morphological similarity; 2) morphological similarity results from recent admixture; 3) shared genetic variation due to incomplete lineage sorting underlies morphological similarity.

Methods and materials

Study system

Stygocapitella is part of the meiofauna, being generally found above the high-water line of sheltered gravel or sandy beaches. To collect individuals, we selected sampling areas based on old records or by assessing beaches using google maps (Google Maps 2017) (Supplementary Table 1; Fig. 1). At each site, we drew a transect from the high-water line to the foot of the dune, digging a 1-meter deep hole every meter starting at the high-water line. In each hole, we collected sediment samples every 15 cm of depth with a volume of about 500 cm^3. Sediment samples were brought to the laboratory and interstitial invertebrates were extracted using the $MgCl_2$ method, and isolated using a dissecting microscope (Westheide and Purschke 1988). After identifying *Stygocapitella*, we collected and preserved these in a ~70% ethanol solution for DNA extraction.

DNA extraction and molecular species barcoding

Since *Stygocapitella westheidei*, *S. subterranea* and *S. josemariobrancoi* are morphologically indistinguishable (Cerca et al. 2020a), we barcoded individual individuals using 16S, 18S, ITS1 and COI as described in Cerca et al. (2020b, a) (Supplementary Table 2 includes NCBI reference-ID). In brief, we extracted DNA from single individuals using either phenol-chloroform or the E.Z.N.A. Tissue DNA Kit (Omega Bio-Tek), and obtained COI (Astrin and Stüben 2008), 18S (Hillis and Dixon 1991), ITS1 (Cerca et al. 2020a), and 16S (Palumbi et al. 1991; Zanol et al. 2010) sequences using PCR. Amplified genetic markers were sequenced by

Sanger-sequencing at Macrogen-Europe. For detailed information on amplification, primer sequences and extraction please see Cerca et al. (2020b, a).

Library preparation and Illumina sequencing

We selected 50 *Stygocapitella josemariobrancoi*, 47 *S. subterranea* and 24 *S. westheidei* for library preparation (Supplementary Table 2). Due to the reduced body size, DNA extractions of *Stygocapitella* yield low concentrations of DNA, therefore, to overcome this problem, we used a combination of whole genome amplification (WGA) (Golombek et al. 2013; de Medeiros and Farrell 2018) followed by a double-digestion Restriction site-Associated DNA sequencing protocol (ddRAD) (Baird et al. 2008; Peterson et al. 2012). To complete the WGA reaction, DNA of a single individual is first denaturated and mixed with random hexamer primers and the Phi29 DNA polymerase (Illustra Genomiphi HY DNA Amplification Kit; GE© Healthcare Life Science). Following the manufacturer's instructions, 2.5µl of template DNA were mixed with 22.5µl of sample buffer, and incubated at 95ºC for three minutes for denaturation. After this, we added 22.5µl of reaction buffer and 2.5µl of enzyme mix to the DNA-sample buffer solution, incubated the solution at 30ºC for four hours for DNA amplification and an enzyme heat-inactivation at 65ºC for ten minutes. DNA was purified using AMPure XP beads, and resuspended in ddH_2O. The concentration of the amplified DNA was determined with Qubit and the fragment size distribution with a fragment-analyzer.

For each individual, 500 ng of amplified DNA was digested in 25 µl including 0.5 µl of each restriction enzyme (Pst-I HF and Mse-I, each 20 units/µl) and 2.5 µl Cut-smart buffer. The digestion reaction was carried out at 37º C for two hours. Digested DNA was purified using Ampure-beads and resuspended in 22 µl ddH_2O, and Illumina adaptors with barcodes were ligated to the digested DNA in a 25 µl reaction including 20.5 µl sample DNA, 1 µl T4 DNA-ligase, 2.5 µl 10X T4 ligase buffer and 1 µl adapter P1/2-mix. This reaction was incubated for 30 minutes at 25ºC, and the enzyme inactivated for 10 minutes at 65ºC. The barcoded libraries were pooled, cleaned using AMPure XP beads, and eluted in 100 µl of ultra-purified water. We ran a size-selection step using Blue Pippin's 100-600 bp cassette (BDF2010) selecting for fragment-length between 300-600 bp followed by cleaning with AMPure XP beads to remove short fragments. The library was amplified in 200 µl including 100 µl Q5 HiFi MasterMix, 5 µl Primer mix and 20 µl DNA, in 18 PCR cycles (initial denaturation: 98ºC for 30s; 18 cycles of 98ºC for 10 seconds, 60ºC

for 15 seconds, 72°C for 15 seconds; and a final elongation of 72°C for 2 minutes). Finally, two cleaning-quantification steps using AMPure XP beads were done, and the libraries were sent for Illumina Sequencing on an Illumina Hi-Seq 4000.

Individual identification and multi-marker phylogeny

Raw 16S, 18S, ITS1 and COI sequences were assembled, and ends were automatically trimmed to remove primers and low-quality ends using Geneious v6.8.1, (Supplementary Table 2). Each consensus sequence was queried against the default NCBI database (nr/nt) using BLAST (Altschul et al. 1990; Camacho et al. 2009) to exclude potential contamination. For each gene, sequences were aligned using mafft v7.310, using a maximum of 1,000 iterations, and the ends of the sequences trimmed until the first position without missing data. The accurate localpair algorithm was used for all genes (Katoh and Standley 2013), with the exception of ITS1, which had a single peak, where the globalpair algorithm was applied as it is optimized for gappy sequences. The dataset was concatenated using FASconCAT v1.1 (Kück and Meusemann 2010), and a partitioned phylogenetic tree was obtained using IQ-tree v1.6.10, by applying 1,000 fastbootstrap replications. Model determination was done automatically by IQ-tree, and it included TIM2+I for ITS1, JC+I for 18S, TN+R2 for 16S and HKY+I for COI. The congruence between these genes, and in the individuals used has previously been determined in Cerca et al. (2020b, a).

De novo RAD assembly

Since no reference genome is available for *Stygocapitella*, we used the *de novo* assembly approach implemented in Stacks v2.2 to identify RAD loci (Rochette and Catchen 2017; Rochette et al. 2019). The first module of Stacks, 'process_radtags', was executed using flags tailored to improve data quality (--clean, --quality, --rescue). To optimize Stacks' parameters, we ran the *de novo* pipeline repeatedly using different -M (mismatch between stacks within individuals) and -n (mismatches between stacks between individuals) values, as suggested by best practices (Paris et al. 2017). The total number of loci resulting from different -M -n values were plotted and analyzed, selecting -M 3 and -n 3 for the final dataset. Populations, as required for the population map, were defined based on the species and sampling site (total of 22 populations - Supplementary Table 1).

Since we observed a considerably high level of missing data in the dataset (>90% missing data), we tested and implemented a new method to improve RADseq datasets. Missing data is

especially problematic in RADseq as it can lead to erroneous inference of population-genetic parameters (Arnold et al. 2013; Gautier et al. 2013; Hodel et al. 2017). However, applying stringent filtering for missing data has been shown to prune parsimonious-informative loci, with best-practices suggesting non-conservative pruning of the data (Huang and Lacey Knowles 2016; Lee et al. 2018; Crotti et al. 2019). To mitigate missing data while avoiding stringent filtering, we applied a novel procedure, which allowed us to retrieve more loci from our data (Cerca et al *submitted*). In brief, we ran Stacks for every population present in the population map – 22 times in total (Supplementary Table 1) – thus lowering phylogenetic distance in the dataset. Since phylogenetic distance (biological origin) and artefacts in generating and processing data can lead to allelic dropout (O'Leary et al. 2018), lowering phylogenetic distance will isolate dropout caused by artefacts in library preparation (e.g. DNA size-selection, low DNA concentrations, poor digestion), and loss of information due to whole genome amplification (de Medeiros and Farrell 2018). For each population, we identified samples with >45% missing loci and removed these from a final analysis (*hereafter* the *clean* dataset). To evaluate how the optimization impacted the final number of loci we compared the number of loci and missingness in the dataset before cleaning (hereafter the *uncleaned* dataset) and in the cleaned dataset using the values of -r 25 (a locus has to be present in at least 25% of individuals comprising a population to be considered) and -p 4 (a locus has to be present in at least 4 populations to be considered). Finally, we included a technical replicate in the dataset (individuals 222 01 and 222 01R), and checked whether it was coherently placed in all the analyses.

Population genomics and phylogenomics

From the clean dataset, we extracted a single nucleotide polymorphism-only dataset (SNPs; hereafter *variant* dataset) and an all-sites dataset (containing non-variant and variant positions; hereafter *all-sites* dataset). Separating the data in these two datasets is necessary to meet the assumptions of some statistical tests which may require the presence of non-variant positions to calculate ratios of variant and non-variant sites. The variant dataset was pruned by selecting -r 50 (a locus has to be present in at least 50% of individuals comprising a population), and -p 8 (a locus has to be part in at least 8 populations) as loci cut-offs, using the 'populations' program included in Stacks, resulting in 4,737 RAD-loci. After this initial round of cleaning, we used vcftools v0.1.13 (Danecek et al. 2011) to further prune the dataset for 5% minimum allele frequency (--

maf), and for mean loci coverage values between 10-100 (--min-meanDP 10 --max-meanDP 100) and removed 12 individuals which had missingness above >90% (--missing-indv; Supplementary Table 2). The combination of coverage filters together with the -M -m optimization procedure mentioned above optimizes the generation of RADseq loci by removing loci which may artificially come together (i.e. repetitive regions). Finally, to decrease the effect of physical linkage in the data, we used a custom BASH shell script which kept only one polymorphism (SNP) per RAD locus, resulting in a final dataset of 3,428 SNPs. Using this dataset, we assessed genetic variation by means of a principal component analysis (PCA), a multi-dimensional scaling (MDS) analysis and an ADMIXTURE analysis. PCA and MDS are model-free approaches to estimate population structure, being complementary as PCA assumes 'mean values' for missing data (i.e. dragging individuals with high missingness to the center) whereas MDS does not. PCA was computed using the R package Adegenet (Jombart and Ahmed 2011) and MDS with plink v1.9 (Chang et al. 2015). ADMIXTURE is a model-oriented approach to determine population structure based on the presence/absence of heterozygotes (Alexander et al. 2009). We ran Admixture assuming 1-6 clusters (K), running a total of 5 replicates for each K, and determined the best K by estimating the cross-validation error (Supplementary Figure 1). Considering the potential for admixture of individuals in sympatry (Figure 1), we used $f3$ statistics, included as part of the Admixtools package, as a direct test for detecting hybridization (Patterson et al. 2012; Peter 2016). These statistics consists of a 3 populations test where a focal population is derived from admixture between the other two populations. When this score is negative, it suggests that admixture likely has occurred. We estimated errors and confidence intervals on the $f3$ statistics by partitioning the dataset into blocks and applying a jackknife bootstrapping. Finally, we inferred species-level divergence by estimating Weir and Cockerham's F_{ST} using vcftools (Weir and Cockerham 1984; Danecek et al. 2011).

The all-sites dataset was obtained by extracting FASTA sequences from Stacks. To run the phylogenomic analysis, we wrote a Perl script to reorganize the data into loci, concatenated all loci in a supermatrix using FasConCat-G (Kück and Longo 2014) and ran a partitioned-tree using IQ-tree v1.6.10 (Nguyen et al. 2015) specifying 1,000 fast bootstrap replications (Chernomor et al. 2016; Hoang et al. 2017), and locus-specific models which were determined as part of the run (Kalyaanamoorthy et al. 2017). To explore the effect of missing data on the tree topology, we ran BaCoCa (Kück and Struck 2014), which runs summary-level statistics on the concatenation matrix

and tree, such as the % of positions with missing data shared by a pair of individuals. Pairwise positive overlap values were plotted to the tree topology using the R package ape (Paradis and Schliep 2018). Additionally, we ran an Unweighted Pair Group Method with Arithmetic mean (UPGMA) tree using only the average % of pairwise shared data per individual (i.e. pairwise percentage of shared data between taxa which do not have an indel, ambiguous character state, or a missing character state). The UPGMA tree was run to understand whether taxa were grouped based on the overall pattern of missing data. We did a species network analysis using SPLITSTREE v4 (Huson and Bryant 2006) to complement phylogenetic inference since the network does not enforce dichotomous branching at each node.

To gauge population-level patterns and diversity, we selected loci from the all-sites dataset without missing-data at the population-level and estimated summary statistics including nucleotide diversity (π), Waterson's estimator of genetic diversity (S) and Tajima's D using DNAsp v6 (Rozas et al. 2017). The selection of sites without missing data is grounded on best-practices as missing data can lead to the under- or overestimation of some of these parameters (Arnold et al. 2013). Importantly, we selected only populations where 3 or more individuals (i.e. > 5 'chromosomes') had data available (Supplementary Table 2).

Finally, we evaluated various demographic scenarios using fastsimcoal2, using the same dataset for the previous analysis which included running fastsimcoal2 (Excoffier et al. 2013). Fastsimcoal2 uses the site-frequency spectrum (SFS) and a coalescent-simulation framework based on an arbitrary user-defined scenario to infer population sizes, strength of gene flow and times of coalescence. Likelihood is then calculated by running the 'best parameters' for each specified scenario multiple times and obtaining the distribution of likelihood estimates. To implement these simulations, we used the phylogeny obtained with *Stygocapitella subterranea* and *S. westheidei* as sister species, and *S. josemariobrancoi* as sister to the remaining two. We defined the following models: no gene flow, ancient gene flow (between *Stygocapitella josemariobrancoi* and the stem lineage of *S. subterranea* and *S. westheidei*), geographic gene flow (similar as the ancient gene flow, but also with modern gene flow between the sympatric *Stygocapitella subterranea* and *S. josemariobrancoi*), modern gene flow (gene flow between all three modern species; note we refer to 'modern' as opposed to 'ancient', that is, currently existing lineages), all gene flow (gene flow between all three species and the two ancestral lineages),

277 modern gene flow only between *S. josemariobrancoi* and *S. subterranea*, modern gene flow only
278 between *S. josemariobrancoi* and *S. westheidei*, modern gene flow only between *S. westheidei* and
279 *S. subterranea*, and gene flow in ancestral times and between *S. subterranea* and *S. westheidei*.
280 When included in the model, gene flow was module as asymmetric. Each model was run 10,000
281 times, and the best fitting scenario was evaluated using likelihood, by running it 100 times.

282 **Results**

283 **Tree of selected molecular markers**

284 We compiled a dataset comprising 4,147 bp (the COI fragment consisted of 629 bp, 16S of
285 548 bp, ITS1 of 1,150 and 18S of 1,817 bp), from which 716 sites were phylogenetic-informative
286 sites. From a total of 69 individuals, we obtained 67 16S sequences, 61 COI sequences, 28 18S
287 sequences and 31 ITS1 sequences. Every species was recovered as monophyletic (Figure 2 A) with
288 bootstrap support values of 100 for *S. josemariobrancoi*, of 86 for *S. subterranea* and of 100 for
289 *S. westheidei* (Figure 2 A). The retrieved tree topology includes *S. westheidei* and *S. subterranea*
290 as sister species. *Stygocapitella josemariobrancoi* as sister to the clade comprising *S. subterranea*
291 and *S. westheidei*. Single gene trees show concordance between markers (Supplementary Figures
292 2-5)

293 **Genomic dataset**

294 We obtained a total of 1,277,919,764□ sequencing reads from two Illumina HiSeq4000
295 lanes. After demultiplexing and cleaning the data with process_radtags, we retained 899,112,800□
296 reads (107,830,588 reads were discarded for having ambiguous barcodes, 270,174,154□ for
297 ambitious RADtags, and 802,222□ for low quality). When comparing the clean and unclean
298 dataset, the approach to lower allelic dropout yielded a substantial increase of the number of loci.
299 In detail, after running Stacks for each population individually, we removed 17 *S. subterranea* out
300 of a total of 47, 7 *S. westheidei* out of 24, and 16 out of 50 for *S. josemariobrancoi* (roughly ~33%
301 of the dataset, Supplementary Table 2). The uncleaned dataset yielded 179,742 loci (55,037,190
302 sites including 628,031 variant sites), whereas the cleaned data yielded 368,696 loci (112,725,106
303 sites including 1,100,431 variant sites). When pruned with common denominators included in the
304 module Populations (-r 50 -p4), the unclean dataset yielded 109,369 loci, and the cleaned yielded
305 272,134 loci. Individual-level missing data was reduced from 84.89% in the uncleaned dataset to

80.79% in the cleaned dataset. We validated this approach by comparing PCA, MDS and phylogenomic trees using both cleaned and the uncleaned dataset (see https://ecoevorxiv.org/47tka). A comprehensive investigation of this strategy including additional datasets will be published in a separate paper (Cerca et al. *submitted*).

Genomic trees and networks

The phylogenomic tree (Figure 2C) shows a slightly different topology from the tree obtained with selected molecular markers. The branches representing *Stygocapitella subterranea*, *S. westheidei*, and *S. josemariobrancoi* have a bootstrap support of 93, 99 and 100, respectively. The tree topology is broadly similar to the selected marker phylogenetic tree, with *S. josemariobrancoi* being sister to the clade comprising *S. subterranea* and *S. westheidei*. However, strictly speaking, none of the species is recovered as monophyletic, since three individuals identified as *S. josemariobrancoi* are not placed with *S. josemariobrancoi*. Specifically, 422 04 from Bristol Channel nests within *S. subterranea*, 422 05 from Bristol Channel nests within *S. westheidei* and 401 03 from St. Efflam is positioned as sister to *S. subterranea* (Figure 2C, individuals denoted by arrows). Importantly, mapping of shared pairwise data in the tree topology suggests that these trends are not driven by missing data, since the branches representing the three aforementioned individuals do not exhibit elevated levels of missing data (Figure 2C). The UPGMA tree, which is solely built on a pairwise matrix of missing-data, shows that *S. subterranea* and *S. josemariobrancoi* are generally separated, interlaced by individuals from *S. westheidei* (Supplementary Figure 6). While this suggests that the three species have different amounts of missing data, the fact that individuals are generally mixed suggests that missing data is not driving phylogenetic reconstruction. For example, the three individuals resulting in a paraphyletic reconstruction are not placed closely to their sister taxa in the tree, therefore indicating that missing data has no influence in the paraphyletic position of these individuals (Supplementary Figure 6).

In the phylogenetic network, *Stygocapitella westheidei* is separated from the remaining two species, occupying a separate and relatively compact area of the network. *Stygocapitella subterranea* is mostly confined to one small section of the network, however, three individuals are very close to the center of the network (398 04, 398 08 and 398 09 from Keitum; Figure 3). In line with the results from the phylogenomic tree, Bristol Channel 422 04, which is identified as part of *S. josemariobrancoi*, is nested within *S. subterranea* in the network. *Stygocapitella*

josemariobrancoi, on the other hand, is clearly stretched and set apart in the network, occupying a large area (Figure 3). While most individuals are nested within a condensed and remote portion of the network, the individuals Bristol Channel 422 05, St Efflam 401 03 and 401 04 lie in an intermediate position between the center of the network and the majority of individuals from *S. josemariobrancoi* (Figure 3). This is broadly in agreement with the phylogenomic tree, which shows Bristol Channel 422 05 nested with *S. westheidei* (Figure 2C) and St. Efflam 401 03 sister to *S. subterranea* (Figure 2C). The distance between most individuals belonging to *S. josemariobrancoi* and the center of the network remaining two species suggests a greater degree of differentiation.

Population structure, differentiation and summary statistics

The PCA separates the three species across the first two principal components, (which together explain 30.4% of the variance; Figure 4A). Three individuals stand out, including Bristol Channel 422 04 (labelled as *S. josemariobrancoi*) which is placed closely with *S. subterranea* individuals, Bristol Channel 422 05 which occupies an intermediate position between *S. westheidei* and *S. josemariobrancoi*, and Lubec 428 02 which is relatively distant from the remaining *S. westheidei* individuals. The multi-dimensional scaling plot, which is less affected by missing data, separates the species into three distinct clusters (MDS; Figure 4B). However, coherently with the previous analyses, we detect several taxa with intermediate positions: Bristol Channel 422 04 (labelled as *S. josemariobrancoi*) is closer to the *S. subterranea* cluster than to the *S. josemariobrancoi*, Hoernum 169 09 (labelled as *S. josemariobrancoi*) in an intermediate position between these two species; Bristol Channel 422 05, St. Efflam 401 04, 401 03, 401 05 (all labelled as *S. josemariobrancoi*) are found in an intermediate position between *S. josemariobrancoi* and *S. westheidei* Lubec 429 02 (labelled as *S. westheidei*) is also distant from the *S. westheidei* cluster, being relatively close to Bristol Channel 422 05 (Figure 4B).

The ADMIXTURE analysis confirms shared genetic signal among species. The most supported cluster size was K = 3 (Supplementary Figure 1) and is plotted in Figure 5. In agreement with the phylogenetic network, the MDS and the PCA, *S. westheidei* is the species with the least amount of admixture, with only 2 individuals sharing a relatively low degree of ancestry with *S. subterranea*. A majority of *S. subterranea* individuals (17 out of 30) share genetic variation with *S. josemariobrancoi*. *S. josemariobrancoi* has 5 individuals which are admixed from *S. westheidei*,

and an individual (Bristol 422 04) identified as having a *S. subterranea* ancestry. Notably, individuals from sympatric areas and belonging to *S. josemariobrancoi* and *S. westheidei* (Hausstrand, Musselburgh, Lubec) show no signal of shared ancestry. However, five *S. subterranea* individuals with shared ancestry belong to two sympatric sites (Hausstrand and Musselburgh). *f*3 statistics were positive, thus suggesting that the observed patterns of admixture are unlikely to be due to recent admixture (Table 1). Notably, two out of three scenarios retrieved Z scores >3 (threshold used for significance), including *S. subterranea* and *S. josemariobrancoi* as source and *S. westheidei* as target, and *S. josemariobrancoi* and *S. westheidei* as sources and *S. subterranea* as target.

Notably, F_{ST} estimates among species are high, thus indicating isolation. Pairwise F_{ST} comparisons were lower between *S. josemariobrancoi* and either of the remaining species: 0.53 for *S. josemariobrancoi* vs *S. subterranea*, 0.492 *S. josemariobrancoi* vs *S. westheidei* and 0.664 for S. *subterranea vs S. westheidei* (Table 2).

Summary statistics suggest that populations of *S. josemariobrancoi* have a higher degree of genetic variation. Waterson's estimate, S, ranges between 2.11-2.39 in *S. subterranea* and between 1.81-2.35 in *S. westheidei*, and between 1.89-6.83 in *S. josemariobrancoi*, with Bristol Channel (S = 4.92), and Gravesend (S = 6.93; Table 3). This is similar when considering nucleotide polymorphisms (π), with *S. subterranea* ranging between 0.002-0.0037, *S. westheidei* between 0.0021-0.0034, but *S. josemariobrancoi* ranging between 0.0026-0.0099 again with Gravesend and Bristol Channel as outliers (Gravesend π = 0.0099, Bristol Channel π = 0.0086; Table 3). Interestingly, sympatric sites do not reveal any signal of higher polymorphism, as it would be expected in scenarios of on-going hybridization. For instance, π = 0.0033 and S = 2.13 for *S. subterranea* in Musselburgh, and π = 0.0045 and S = 2.49 for *S. josemariobrancoi* in Musselburgh. Hausstrand, for which we were only able to obtain data for *S. josemariobrancoi* retrieved a π = 0.0038 and a S = 2.55, while the population Lubec of *S. westheidei* shows π = 0.0029 and S = 2.15. Tajima's D excludes the possibility for bottlenecks, as none of the populations exhibits significant Tajima's D (i.e. values below -2 or above +2; Table 3).

Absence of recent admixture is also supported by the simulation of demographic scenarios (Figure 6), as two of the top three most supported scenarios suggest no recent gene flow: ancient gene flow (i.e. gene flow between the two ancestral branches), no gene flow. The most supported

scenario, however, suggests there has been gene flow between *S. subterranea* and *S. westheidei*. This scenario seems unlikely, since the estimated time of coalescence of 3,759 generations ago (presumably *Stygocapitella* has a generation time of a single year) between *S. subterranea* and *S. westheidei*, and 31,853 generations for *S. josemariobrancoi* and the ancestral lineage for *S. subterranea* and *S. westheidei*. These numbers are clearly at odds with previous evidence suggesting these lineages diverged millions of years ago (Struck et al. 2017; Cerca et al. 2020a). The ancient gene flow scenario includes estimates of 1,130,483 generations for the first coalescent event, and 12,816,687 generations for the second coalescent event. No gene flow scenario estimates 205,937 and 7,482,922 generations ago (Supplementary Material). The least supported scenarios generally involved gene flow between modern lineages (Figure 6).

Discussion

Morphological similarity through extended periods of times, or stasis, has been hypothesized to occur under three possible scenarios underlied by genetics: homogenous genetic variation (due to e.g. ILS, hybridization), genetic constraints (e.g. pleiotropy), and lack of genetic variation (e.g. bottlenecks and founder effects) (Futuyma 2010). While our sampling design does not account for genetic constraints, we study the evolutionary history of *Stygocapitella* species seeking to determine signals of loss of genetic variation or shared genetic variance. We find that the three morphologically similar *Stygocapitella* species herein studied share genetic variation and exclude the possibility of recent bottlenecks or recent admixture. Demographic and admixture analysis reveal signatures of incomplete lineage sorting and possibly ancestral admixture during the divergence of these three species. We discuss the possible implications of these processes to the genomic underpinnings of indistinguishable morphology among cryptic species.

Whole genome amplification and the generation of RADseq data

We show that WGA combined with RAD sequencing may become an important tool for microscopic eukaryote genomics. RADseq library preparation typically requires 200-500 ng of DNA per individual, yet DNA extraction of a single *Stygocapitella* individual typically yields 10-100 ng of DNA, thus representing a challenge to obtain genome-level data. One potential solution is to pool individuals. However, pooling may not be ideal when dealing with morphologically similar species, especially when they occur in sympatry, as observed in *Stygocapitella*, since the

identification of individuals based solely on morphology may be impossible. Arguably, one of the major advantages of RADseq is to open up population genomics and phylogenomics as approaches for non-model systems at an affordable cost. In such systems, experimental designs may benefit from the inclusion of the largest number of individuals possible, which encompass the whole spectrum of populations or species to determine species boundaries, phylogeography, population structure and the phylogeny. Pooling individuals from different species or populations together may lead to an incorrect inference of the phylogeny when species boundaries are not known, but also skew allelic variation. Consequently, pooling of individuals may result in difficulties during data processing and interpretation, and may require extra efforts such as barcoding of individuals before pooling. In the view of these challenges, we optimized and applied a whole-genome amplification protocol to obtain genome level data, thus confirming its potential for population genomic-inference and phylogenetics (de Medeiros and Farrell 2018, 2019).

Bottlenecks, meiofaunal dispersal and morphological similarity

The few phylogeographic studies available for meiofaunal organisms have generally detected founder effects and bottlenecks, and have discussed how colonization dynamics may be determined by a series of bottlenecks (Casu and Curini-Galletti 2006; Derycke et al. 2007; Andrade et al. 2011), however, we find no evidence for bottlenecks in this dataset when using summary statistics and Tajima's D. Evidence for the prevalence of bottlenecks in meiofauna has been further supported by experimental evidence which showed that colonization of new areas may be characterized by founder effects and bottlenecks, which, in turn, are expected to shape the genetic differentiation of meiofaunal populations (Derycke et al. 2007, 2013). Broadly, this follows hypotheses on marine-invertebrate biogeography which suggests that repeated extinction and recolonization dynamics may be involved in shaping genetic differentiation in populations and species (Andrade et al. 2011; Derycke et al. 2013). We find no indication of bottlenecks in *Stygocapitella,* as suggested by non-significant Tajima's D values (Table 3), even though that part of the sampling distribution of *Stygocapitella* included areas which were glaciated only 10,000 years ago (Wares and Cunningham 2001). Two possibilities may explain this scenario and support our findings. First, the hypothesis that meiofauna disperse through a series of bottlenecks may require more evidence. Indeed, when scoring a total of 752 papers, we could only detect 48 studies focusing on biogeography and 7 on evolutionary biology (including population genetics) (Cerca

et al. 2018), thus suggesting that meiofaunal biogeography is in its early days and more studies are needed for more solid conclusions. This hypothesis may also be at odds with evidence that meiofauna may be, indeed, good dispersers (reviewed in Cerca et al. 2018). Even if dispersal is carried by only a limited group of individuals, concomitant with the idea of a founder effect and bottleneck colonization, the dispersal of more organisms from 'source populations' (multiple waves of dispersal) through time would eventually homogenize genetic variation in newly colonized areas. Second, to the best of our knowledge, this is the first work to focus on population-genomic level data in meiofauna. Typically, works have focused on sequencing a limited combination of mitochondrial and nuclear genes (e.g. (Derycke et al. 2005, 2007, 2008; Kieneke et al. 2012; Leasi and Norenburg 2014). While non-recombining data, such as mitochondrial markers, may provide an ideal indication for the occurrence of bottlenecks, these effects should be confirmed on complementary genomic regions. For instance, using the 16S mitochondrial marker, we previously detected single haplotypes in populations of *S. subterreanea* or *S. josemariobrancoi*. These populations had a statistically significant Tajima's D (*S. josemariobrancoi* individuals from Bristol Channel; *S. subterranea* individuals from Glenancross) (Cerca et al. 2020b). While this pattern was in conflict with that of the nuclear ITS1 (Cerca et al. 2020a), it is further rejected when using genome-level data, which provides a more comprehensive, and independent, assessment of genomic variance. This suggests that the dispersal-by-bottlenecks idea in meiofauna warrants more data, and that biogeography of meiofauna will benefit from more genomic studies.

Overall, we suggest that morphological similarity in *Stygocapitella* is unlikely to result from the lack of standing genetic variation due to re-occurring bottlenecks. Under this hypothesis, it is expected that bottlenecks reduce genetic variation, which will in turn limit morphological evolution, thus leading to stasis (Futuyma 2010). Given the lack of evidence for recent bottlenecks in *Stygocapitella*, this does not seem plausible. In addition to the evidence for the lack of recent bottlenecks, the fact that the remaining 8 *Stygocapitella* species live in similar habitats and are distributed throughout the world (Cerca et al. 2020a) indirectly suggests that bottlenecks may not be typical in the evolutionary history of the group.

Evidence for Incomplete Lineage Sorting and Admixture

We find clear evidence for shared genetic variation in *Stygocapitella*, which likely results from shared genetic variation. The most conspicuous evidence for this comes from the admixture

analysis, which clearly demonstrates admixed populations in the three species (Figure 5). This evidence is further supported by individuals with intermediate positions in the MDS – a test which is robust to missing data (Figure 4). Despite this evidence, we reject recent admixture based on several evidences. First, we obtained no evidence for admixture when using F-statistics, since we find only positive F-values. Second, evidence from summary statistics contributes to rejecting on-going geneflow, as sympatric populations (Lubec in the USA, Musselburgh in Scotland, Hausstrand in Germany) do not show higher levels of heterozygosity. It would be expected that hybridization occurs in populations where individuals occur in sympatry since individuals of different species are found in the same sediment sample in close proximity (volume ranging from 50-500 cm^3). Third, admixture could generate incongruence between mitochondrial and nuclear markers (Melo-Ferreira et al. 2012; Sloan et al. 2017), which is not seen in individual trees (Supplementary Figures 2-5). Fourth, demographic scenarios including recent admixture and on-going gene flow generally underperform. However, one of the most supported scenarios involves gene flow in the terminal branches (gene flow in 'sub – west lineages'). We discard the possibility of this scenario since it suggests coalescent times times of 3,759 and 31,853 generations or years (1 generation is expected to be 1 year, Günter Purschke pers. comm)], not compatible with estimates of the splitting age of the three *Stygocapitella* species may have been ~5-30 million years ago (Cerca et al. 2020b). While we admit this is speculative, future studies are necessary to confidently dissect and determine the role of gene flow in the system. For example, these studies will benefit from using whole-genome data to determine whether interspecific divergence in regions of the genome show gene-species tree discordance, thereby dissecting ILS and hybridization (Joly et al. 2009; Giska et al. 2019). In sum, to the extent that we can speculate, our data suggests that shared genetic variance is more likely explained by ancient geneflow or incomplete lineage sorting. However, an "ancient admixture" scenario and ILS may not be completely discernible given the relatively low number of markers obtained by RADseq (~4,000 SNPs) and high missing data in the dataset.

Evidence for ancient admixture or incomplete lineage sorting is further seen in the phylogenomic analysis. Phylogenetic approaches, which seek to reconstruct the evolutionary history of lineages, often fail to resolve the evolutionary history and the 'true tree-topology' when the taxa in question have high rates of incomplete lineage sorting or admixture (Kubatko and Degnan 2007; Degnan and Rosenberg 2009), but incongruence may also result from tree-building

errors, paralogy or horizontal gene transfer (Scornavacca and Galtier 2017). We discard tree-building errors based on the following evidence. First, individuals with intermediate positions in the PCA and MDS correspond to those causing paraphyly in the trees. Second, when exploring the effects of missing data through a) labelling the tree with % of missing data (Figure 2); and b) constructing a cladogram based only on the shear % of missing data (i.e. UPGMA tree, Supplementary Figure 6); we find the placement of intermediate individuals is not guided by missing data. Should missing data determine their placement, we would expect these specimens to nest in close proximity in the UPGMA tree. Finally, in the phylogenetic network, the individuals which are also far removed from the remaining *S. josemariobrancoi* individuals, occupying central positions or being paraphyletic in the phylogenetic network correspond to those paraphyletic in the tree and in intermediate positions in the PCA and MDS.

In sum, incomplete lineage sorting is known to contribute to levels of shared variation among species (Pease et al. 2016; Malinsky et al. 2018; Edelman et al. 2019), even at deep evolutionary levels (Song et al. 2015; Suh et al. 2015). The development of tools which employ the substantial amount of modern genomic data has allowed separating cases of ILS and ancient admixture, showing that ancient hybridization can have a strong impact in the levels of shared variation among species complexes (Malinsky et al. 2018; Li et al. 2019; Taylor and Larson 2019; Ferreira et al. 2020), even after several million years of divergence (Barth et al. 2020). Future work should employ multispecies-network methods or coalescent simulations (Joly et al. 2009) to determine the relative role of ILS and ancient admixture. However, it does not seem unlikely that both processes might have thus contributed to levels of shared variation across 5-30 millions of the divergence of *Stygocapitella* (Cerca 2020).

Incomplete lineage sorting and morphological similarity

The debate on morphological similarity is slowly shifting from ‘are cryptic species an artefact of systematics?’ to ‘what are the causes underlying morphological similarity?’, following the evidence that speciation is not necessarily accompanied by morphological divergence (Wada et al. 2013; Swift et al. 2016; Cerca et al. 2020b). We have previously argued that the study of morphological similarity will benefit from predictions, models, and evidence from paleontological stasis (Cerca et al. 2020a), which suggest that stasis may result from constraints, selective pressures on physiology and/or behaviour, stabilizing selection, niche conservatism (Hansen and Houle

2004; Estes and Arnold 2007; Futuyma 2010). While similarity in different cryptic species complexes may stem from different causes, morphological similarity in the three studied *Stygocapitella* species complex is likely associated with homogeneous genetic variation caused by incomplete lineage sorting and ancestral admixture that occurred during the divergence of the complex (Futuyma 2010). In such a scenario, it is expected that patterns of genetic variation remain similar for the species, thus resulting in the retention of symplesiomorphic morphological states (Futuyma 2010) and in the deceleration of morphological evolution (Cerca et al. 2020b). In any case, future works using whole-genome data are necessary to, for example, detect if regions affected by incomplete lineage sorting and gene flow are disproportionally enriched for genes that usually contribute for morphological divergence in closely related taxa. These works should also employ more variant-level data to confirm the patterns herein obtained.

Conclusions

The increasing discovery of cryptic species has led to heated debates in systematics, mostly lacking an integration in an evolutionary framework. Here, we tested the hypotheses that morphological similarity may own to reduced genetic variation (bottlenecks, founder effects), recent admixture (shared genetic variation), or incomplete lineage sorting. We found that morphological similarity in the three morphologically similar *Stygocapitella* species may own to incomplete lineage sorting underlying shared genetic variation. Future works should focus on understanding whether reduced genetic variation or shared genetic variation underlies morphological similarity in other systems.

Acknowledgements

JC is grateful to Tim Worsfold, Andy Mackie, Henning Reiss, Lis Jørgensen for laboratory space in the UK and Norway. We thank Audun Schrøder-Nielsen and Lisbeth Thorbek for assistance in laboratory work, and Inês Modesta for fieldwork support. We acknowledge the use of Norwegian national infrastructure for high-performance computing and storage via the projects NN9408K and NS9408K, respectively. Fieldwork was partly supported by a Den Grevelige Hjelmstjerne-Rosencroneske Stiftelse ved UiO (JC), and THS was partly supported by the EU Assemble program. A UiO:LifeScience internationalization support and a Godfrey Hewitt mobility award allowed JC to visit Julian Catchen at the UIUC. MSF was supported by POPH-

QREN funds from ESF and Portuguese MCTES/FCT (PD/BD/108131/2015 PhD grant in the scope of BIODIV PhD programme at Faculty of Sciences, University of Porto) and NSF (OIA-1736249). This is NHM genomics laboratory contribution **XX**.

Author contributions

JCe, MDM, THS designed this study. JCe and THS collected organisms in the field. JCe extracted DNA and prepared RADseq libraries. JCe did data analysis with support of MR (population genomics), JCa (RADseq), AR-C (RADseq), MSF (ILS), and THS (phylogenetics). JCe drafted the manuscript, which was read, commented on and approved by all the remaining authors.

References

Alexander DH, Novembre J, Lange K (2009) Fast model-based estimation of ancestry in unrelated individuals. Genome Res 19:1655–1664. https://doi.org/10.1101/gr.094052.109

Altschul SF, Gish W, Miller W, et al (1990) Basic local alignment search tool. J Mol Biol 215:403–410. https://doi.org/10.1016/S0022-2836(05)80360-2

Andrade SCS, Norenburg JL, Solferini VN (2011) Worms without borders: Genetic diversity patterns in four Brazilian *Ototyphlonemertes* species (Nemertea, Hoplonemertea). Mar Biol 158:2109–2124. https://doi.org/10.1007/s00227-011-1718-3

Arnold B, Corbett-Detig RB, Hartl D, Bomblies K (2013) RADseq underestimates diversity and introduces genealogical biases due to nonrandom haplotype sampling. Mol Ecol 22:3179–3190. https://doi.org/10.1111/mec.12276

Astrin JJ, Stüben PE (2008) Phylogeny in cryptic weevils: Molecules, morphology and new genera of western Palaearctic Cryptorhynchinae (Coleoptera: Curculionidae). Invertebr Syst 22:503–522. https://doi.org/10.1071/IS07057

Baird NA, Etter PD, Atwood TS, et al (2008) Rapid SNP discovery and genetic mapping using sequenced RAD markers. PLoS One 3:e3376. https://doi.org/10.1371/journal.pone.0003376

Barth JMI, Gubili C, Matschiner M, et al (2020) Stable species boundaries despite ten million years of hybridization in tropical eels. Nat Commun 11:1–13.

https://doi.org/10.1038/s41467-020-15099-x

Bernardo J (2011) A critical appraisal of the meaning and diagnosability of cryptic evolutionary diversity, and its implications for conservation in the face of climate change. Clim Chang Ecol Syst 380–438. https://doi.org/10.1017/CBO9780511974540.019

Bickford D, Lohman DJ, Sodhi NS, et al (2007) Cryptic species as a window on diversity and conservation. Trends Ecol Evol 22:148–155. https://doi.org/10.1016/j.tree.2006.11.004

Camacho C, Coulouris G, Avagyan V, et al (2009) BLAST+: Architecture and applications. BMC Bioinformatics 10:1–9. https://doi.org/10.1186/1471-2105-10-421

Casu M, Curini-Galletti M (2006) Genetic evidence for the existence of cryptic species in the mesopsammic flatworm *Pseudomonocelis ophiocephala* (Rhabditophora: Proseriata). Biol J Linn Soc 87:553–576. https://doi.org/10.1111/j.1095-8312.2006.00588.x

Cerca J, Meyer C, Purschke G, Struck TH (2020a) Delimitation of cryptic species drastically reduces the geographical ranges of marine interstitial ghost-worms (Stygocapitella; Annelida, Sedentaria). Mol Phylogenet Evol 143:106663. https://doi.org/10.1016/j.ympev.2019.106663

Cerca J, Meyer C, Stateczny D, et al (2020b) Deceleration of morphological evolution in a cryptic species complex and its link to paleontological stasis. Evolution (N Y) n/a:1–16. https://doi.org/10.1111/evo.13884

Cerca J, Purschke G, Struck TH (2018) Marine connectivity dynamics: clarifying cosmopolitan distributions of marine interstitial invertebrates and the meiofauna paradox. Mar Biol 165:123. https://doi.org/10.1007/s00227-018-3383-2

Chang CC, Chow CC, Tellier LCAM, et al (2015) Second-generation PLINK: Rising to the challenge of larger and richer datasets. Gigascience 4:1–16. https://doi.org/10.1186/s13742-015-0047-8

Chenuil A, Cahill AE, Délémontey N, et al (2019) Problems and questions posed by cryptic species. A framework to guide future studies. pp 77–106

627 Chernomor O, Von Haeseler A, Minh BQ (2016) Terrace aware data structure for phylogenomic
628 inference from supermatrices. Syst Biol 65:997–1008.
629 https://doi.org/10.1093/sysbio/syw037

630 Crotti M, Barratt CD, Loader SP, et al (2019) Causes and analytical impacts of missing data in
631 RADseq phylogenetics: Insights from an African frog (Afrixalus). Zool Scr 48:157–167.
632 https://doi.org/10.1111/zsc.12335

633 Danecek P, Auton A, Abecasis G, et al (2011) The variant call format and VCFtools.
634 Bioinformatics 27:2156–2158. https://doi.org/10.1093/bioinformatics/btr330

635 De León GPP, Nadler SA (2010) What we don't recognize can hurt us: A plea for awareness
636 about cryptic species. J Parasitol 96:453–464. https://doi.org/10.1645/GE-2260.1

637 de Medeiros BAS, Farrell BD (2018) Whole genome amplification in double-digest RAD-seq
638 results in adequate libraries but fewer sequenced loci. PeerJ.
639 https://doi.org/10.7717/peerj.5089

640 de Medeiros BAS, Farrell BD (2019) Evaluating species interactions as a driver of phytophagous
641 insect divergence. bioRxiv. https://doi.org/10.1101/842153

642 Degnan JH, Rosenberg NA (2009) Gene tree discordance, phylogenetic inference and the
643 multispecies coalescent. Trends Ecol Evol 24:332–340.
644 https://doi.org/10.1016/j.tree.2009.01.009

645 Derycke S, Backeljau T, Moens T (2013) Dispersal and gene flow in free-living marine
646 nematodes. Front Zool 10:1. https://doi.org/10.1186/1742-9994-10-1

647 Derycke S, Remerie T, Backeljau T, et al (2008) Phylogeography of the *Rhabditis* (Pellioditis)
648 marina species complex: Evidence for long-distance dispersal, and for range expansions and
649 restricted gene flow in the northeast Atlantic. Mol Ecol 17:3306–3322.
650 https://doi.org/10.1111/j.1365-294X.2008.03846.x

651 Derycke S, Remerie T, Vierstraete A, et al (2005) Mitochondrial DNA variation and cryptic
652 speciation within the free-living marine nematode *Pellioditis marina*. Mar Ecol Prog Ser
653 300:91–103. https://doi.org/10.3354/meps300091

654 Derycke S, Vynckt R Van, Vanoverbeke J, et al (2007) Colonization patterns of Nematoda on
655 decomposing algae in the estuarine environment: Community assembly and genetic
656 structure of the dominant species *Pellioditis marina*. Limnol Oceanogr 52:992–1001.
657 https://doi.org/10.4319/lo.2007.52.3.0992

658 Dornburg A, Federman S, Eytan RI, Near TJ (2016) Cryptic species diversity in sub-Antarctic
659 islands: A case study of Lepidonotothen. Mol Phylogenet Evol 104:32–43.
660 https://doi.org/10.1016/j.ympev.2016.07.013

661 Dufresnes C, Strachinis I, Suriadna N, et al (2019) Phylogeography of a cryptic speciation
662 continuum in Eurasian spadefoot toads (Pelobates). Mol Ecol 3257–3270.
663 https://doi.org/10.1111/mec.15133

664 Edelman NB, Frandsen PB, Miyagi M, et al (2019) Genomic architecture and introgression
665 shape a butterfly radiation. Science (80-) 599:594–599

666 Eldredge N, Gould SJ (1972) Punctuated Equilibria: An alternative to phylogetic gradualism. In:
667 Schopf TJM (ed) Models in paleobiology. Freeman, Cooper and Co., San Francisco., pp
668 82–115

669 Erlank E, Koekemoer LL, Coetzee M (2018) The importance of morphological identification of
670 African anopheline mosquitoes (Diptera: Culicidae) for malaria control programmes. Malar
671 J 17:1–7. https://doi.org/10.1186/s12936-018-2189-5

672 Estes S, Arnold SJ (2007) Resolving the paradox of stasis: models with stabilizing selection
673 explain evolutionary divergence on all timescales. Am Nat 169:227–244.
674 https://doi.org/10.1086/510633

675 Ewing G, Hermisson J (2010) MSMS: A coalescent simulation program including
676 recombination, demographic structure and selection at a single locus. Bioinformatics
677 26:2064–2065. https://doi.org/10.1093/bioinformatics/btq322

678 Excoffier L, Dupanloup I, Huerta-Sánchez E, et al (2013) Robust Demographic Inference from
679 Genomic and SNP Data. PLoS Genet 9:. https://doi.org/10.1371/journal.pgen.1003905

680 Ferreira MS, Jones MR, Callahan CM, et al (2020) The legacy of recurrent introgression during

681 the radiation of hares. bioRxiv

682 Fišer C, Robinson CT, Malard F (2018) Cryptic species as a window into the paradigm shift of
683 the species concept. Mol Ecol 27:613–635. https://doi.org/10.1111/mec.14486

684 Futuyma DJ (2010) Evolutionary constraint and ecological consequences. Evolution (N Y)
685 64:1865–1884. https://doi.org/10.1111/j.1558-5646.2010.00960.x

686 Gautier M, Gharbi K, Cezard T, et al (2013) The effect of RAD allele dropout on the estimation
687 of genetic variation within and between populations. Mol Ecol 22:3165–3178.
688 https://doi.org/10.1111/mec.12089

689 Giska I, Farelo L, Pimenta J, et al (2019) Introgression drives repeated evolution of winter coat
690 color polymorphism in hares. Proc Natl Acad Sci U S A 116:24150–24156.
691 https://doi.org/10.1073/pnas.1910471116

692 Golombek A, Tobergte S, Nesnidal MP, et al (2013) Mitochondrial genomes to the rescue –
693 Diurodrilidae in the myzostomid trap. Mol Phylogenet Evol 68:312–326

694 Gould SJ (2002) The structure of evolutionary theory

695 Hansen TF, Houle D (2004) Evolvability, stabilizing selection, and the problem of stasis. In:
696 Pigliucci M, Preston K (eds) Phenotypic integration: studying the ecology and evolution of
697 complex phenotypes. Oxford University Press, New York, pp 130–154

698 Hillis DM, Dixon MT (1991) Ribosomal DNA: Molecular evolution and phylogenetic inference.
699 Q Rev Biol 66:411–453

700 Hoang DT, Chernomor O, von Haeseler A, et al (2017) Ufboot2: Improving the ultrafast
701 bootstrap approximation. 35:518–522. https://doi.org/10.5281/zenodo.854445

702 Hodel RGJ, Chen S, Payton AC, et al (2017) Adding loci improves phylogeographic resolution
703 in red mangroves despite increased missing data: Comparing microsatellites and RAD-Seq
704 and investigating loci filtering. Sci Rep 7:1–14. https://doi.org/10.1038/s41598-017-16810-
705 7

706 Huang H, Lacey Knowles L (2016) Unforeseen consequences of excluding missing data from

next-generation sequences: Simulation study of rad sequences. Syst Biol 65:357–365. https://doi.org/10.1093/sysbio/syu046

Huson DH, Bryant D (2006) Application of phylogenetic networks in evolutionary studies. Mol Biol Evol 23:254–267. https://doi.org/10.1093/molbev/msj030

Joly S, McLenachan PA, Lockhart PJ (2009) A statistical approach for distinguishing hybridization and incomplete lineage sorting. Am Nat 174:. https://doi.org/10.1086/600082

Jombart T, Ahmed I (2011) adegenet 1.3-1: New tools for the analysis of genome-wide SNP data. Bioinformatics 27:3070–3071. https://doi.org/10.1093/bioinformatics/btr521

Kalyaanamoorthy S, Minh BQ, Wong TKF, et al (2017) ModelFinder: Fast model selection for accurate phylogenetic estimates. Nat Methods 14:587–589. https://doi.org/10.1038/nmeth.4285

Katoh K, Standley DM (2013) MAFFT multiple sequence alignment software version 7: Improvements in performance and usability. Mol Biol Evol 30:772–780. https://doi.org/10.1093/molbev/mst010

Kieneke A, Martínez Arbizu PM, Fontaneto D (2012) Spatially structured populations with a low level of cryptic diversity in European marine Gastrotricha. Mol Ecol 21:1239–54. https://doi.org/10.1111/j.1365-294X.2011.05421.x

Knowlton N (1993) Sibling species in the sea. Annu Rev Ecol Syst 24:189–216

Korshunova T, Martynov A, Bakken T, Picton B (2017) External diversity is restrained by internal conservatism: New nudibranch mollusc contributes to the cryptic species problem. Zool Scr 46:683–692. https://doi.org/10.1111/zsc.12253

Kubatko LS, Degnan JH (2007) Inconsistency of phylogenetic estimates from concatenated data under coalescence. Syst Biol 56:17–24. https://doi.org/10.1080/10635150601146041

Kück P, Longo GC (2014) FASconCAT-G: Extensive functions for multiple sequence alignment preparations concerning phylogenetic studies. Front Zool 11:1–8. https://doi.org/10.1186/s12983-014-0081-x

733 Kück P, Meusemann K (2010) FASconCAT: Convenient handling of data matrices. Mol
734 Phylogenet Evol 56:1115–1118. https://doi.org/10.1016/j.ympev.2010.04.024

735 Kück P, Struck TH (2014) BaCoCa - A heuristic software tool for the parallel assessment of
736 sequence biases in hundreds of gene and taxon partitions. Mol Phylogenet Evol 70:94–98.
737 https://doi.org/10.1016/j.ympev.2013.09.011

738 Lavoué S, Miya M, Arnegard ME, et al (2011) Remarkable morphological stasis in an extant
739 vertebrate despite tens of millions of years of divergence. Proc Biol Sci / R Soc 278:1003–
740 1008. https://doi.org/10.1098/rspb.2010.1639

741 Leasi F, Norenburg JL (2014) The necessity of DNA taxonomy to reveal cryptic diversity and
742 spatial distribution of meiofauna, with a focus on Nemertea. PLoS One 9:.
743 https://doi.org/10.1371/journal.pone.0104385

744 Lee CE, Frost BW (2002) Morphological stasis in the Eurytemora affinis species complex
745 (Copepoda: Temoridae). In: Hydrobiologia. pp 111–128

746 Lee KM, Kivela SM, Ivanov V, et al (2018) Information Dropout Patterns in Restriction Site
747 Associated DNA Phylogenomics and a Comparison with Multilocus Sanger Data in a
748 Species-Rich Moth Genus. Syst Biol 1–15. https://doi.org/10.1093/sysbio/syy029

749 Li G, Figueiró H V., Eizirik E, et al (2019) Recombination-Aware Phylogenomics Reveals the
750 Structured Genomic Landscape of Hybridizing Cat Species. Mol Biol Evol 36:2111–2126.
751 https://doi.org/10.1093/molbev/msz139

752 Malinsky M, Svardal H, Tyers AM, et al (2018) Whole-genome sequences of Malawi cichlids
753 reveal multiple radiations interconnected by gene flow. Nat Ecol Evol 2:1940–1955.
754 https://doi.org/10.1038/s41559-018-0717-x

755 Maps G (2017) Google Maps [online]

756 Melo-Ferreira J, Boursot P, Carneiro M, et al (2012) Recurrent introgression of mitochondrial
757 DNA among hares (lepus spp.) revealed by species-tree inference and coalescent
758 simulations. Syst Biol 61:367–381. https://doi.org/10.1093/sysbio/syr114

759 Nadler SA, De Len GPP (2011) Integrating molecular and morphological approaches for
760 characterizing parasite cryptic species: Implications for parasitology. Parasitology
761 138:1688–1709. https://doi.org/10.1017/S003118201000168X

762 Nguyen LT, Schmidt HA, Von Haeseler A, Minh BQ (2015) IQ-TREE: A fast and effective
763 stochastic algorithm for estimating maximum-likelihood phylogenies. Mol Biol Evol
764 32:268–274. https://doi.org/10.1093/molbev/msu300

765 Novo M, Almodóvar A, Fernández R, et al (2010) Cryptic speciation of hormogastrid
766 earthworms revealed by mitochondrial and nuclear data. Mol Phylogenet Evol 56:507–512.
767 https://doi.org/10.1016/j.ympev.2010.04.010

768 Novo M, Almodóvar A, Fernández R, et al (2012) Appearances can be deceptive: Different
769 diversification patterns within a group of mediterranean earthworms (Oligochaeta,
770 Hormogastridae). Mol Ecol 21:3776–3793. https://doi.org/10.1111/j.1365-
771 294X.2012.05648.x

772 O'Leary SJ, Puritz JB, Willis SC, et al (2018) These aren't the loci you'e looking for: Principles
773 of effective SNP filtering for molecular ecologists. Mol Ecol 27:3193–3206.
774 https://doi.org/10.1111/mec.14792

775 Palumbi S, Martin A, Romano S, et al (1991) The simple fool's guide to PCR, version 2.

776 Pante E, Puillandre N, Viricel A, et al (2015) Species are hypotheses: avoid connectivity
777 assessments based on pillars of sand. Mol Ecol 24:525–544.
778 https://doi.org/10.1111/mec.13048

779 Paradis E, Schliep K (2018) Ape 5.0: An environment for modern phylogenetics and
780 evolutionary analyses in R. Bioinformatics 35:526–528.
781 https://doi.org/10.1093/bioinformatics/bty633

782 Paris JR, Stevens JR, Catchen JM (2017) Lost in parameter space: a road map for stacks.
783 Methods Ecol Evol 8:1360–1373. https://doi.org/10.1111/2041-210X.12775

784 Patterson N, Moorjani P, Luo Y, et al (2012) Ancient admixture in human history. Genetics
785 192:1065–1093. https://doi.org/10.1534/genetics.112.145037

786 Pease JB, Haak DC, Hahn MW, Moyle LC (2016) Phylogenomics Reveals Three Sources of
787 Adaptive Variation during a Rapid Radiation. PLoS Biol 14:1–24.
788 https://doi.org/10.1371/journal.pbio.1002379

789 Pérez-Ponce de León G, Poulin R (2016) Taxonomic distribution of cryptic diversity among
790 metazoans: not so homogeneous after all. Biol Lett 12:20160371.
791 https://doi.org/10.1098/rsbl.2016.0371

792 Peter BM (2016) Admixture, population structure, and f-statistics. Genetics 202:1485–1501.
793 https://doi.org/10.1534/genetics.115.183913

794 Peterson BK, Weber JN, Kay EH, et al (2012) Double digest RADseq: An inexpensive method
795 for de novo SNP discovery and genotyping in model and non-model species. PLoS One 7:.
796 https://doi.org/10.1371/journal.pone.0037135

797 Pfenninger M, Schwenk K (2007) Cryptic animal species are homogeneously distributed among
798 taxa and biogeographical regions. BMC Evol Biol 7:121. https://doi.org/10.1186/1471-
799 2148-7-121

800 Rochette N, Rivera-Colón A, Catchen JM (2019) Stacks2: Analytical methods for paired-end
801 sequencing improve RADseq-based population genomics. Mol Ecol.
802 https://doi.org/10.1111/mec.15253

803 Rochette NC, Catchen JM (2017) Deriving genotypes from RAD-seq short-read data using
804 Stacks. Nat Protoc 12:2640–2659. https://doi.org/10.1038/nprot.2017.123

805 Rozas J, Ferrer-Mata A, Sánchez-DelBarrio JC, et al (2017) DnaSP 6: DNA sequence
806 polymorphism analysis of large data sets. Mol Biol Evol 34:3299–3302.
807 https://doi.org/10.1093/molbev/msx248

808 Santamaria CA, Mateos M, Dewitt TJ, Hurtado LA (2016) Constrained body shape among
809 highly genetically divergent allopatric lineages of the supralittoral isopod Ligia occidentalis
810 (Oniscidea). Ecol Evol 6:1537–1554. https://doi.org/10.1002/ece3.1984

811 Scornavacca C, Galtier N (2017) Incomplete lineage sorting in mammalian phylogenomics. Syst
812 Biol 66:112–120. https://doi.org/10.1093/sysbio/syw082

Sloan DB, Havird JC, Sharbrough J (2017) The on-again, off-again relationship between mitochondrial genomes and species boundaries. Mol Ecol 26:2212–2236. https://doi.org/10.1111/mec.13959

Smith MA, Eveleigh ES, McCann KS, et al (2011) Barcoding a quantified food web: Crypsis, concepts, ecology and hypotheses. PLoS One 6:. https://doi.org/10.1371/journal.pone.0014424

Song S, Liu L, Edwards S V, Wu S (2015) Erratum: Resolving conflict in eutherian mammal phylogeny using phylogenomics and the multispecies coalescent model (Proceedings of the National Academy of Sciences of the United States of America (2012) 109 (14942-14947) (DOI:10.1073/pnas.1211733109)). Proc Natl Acad Sci U S A 112:E6079. https://doi.org/10.1073/pnas.1518753112

Struck TH, Cerca J (2019) Cryptic species and their Evolutionary significance. eLS 1–9. https://doi.org/10.1002/9780470015902.a0028292

Struck TH, Feder JL, Bendiksby M, et al (2018) Finding evolutionary processes hidden in cryptic species. Trends Ecol Evol 1–11. https://doi.org/10.1016/j.tree.2017.11.007

Suh A, Smeds L, Ellegren H (2015) The dynamics of incomplete lineage sorting across the ancient adaptive radiation of neoavian birds. PLoS Biol 13:1–18. https://doi.org/10.1371/journal.pbio.1002224

Swift HF, Daglio LG, Dawson MN (2016) Three routes to crypsis: stasis, convergence, and parallelism in the *Mastigias* species complex (Scyphozoa, Rhizostomeae). Mol Phylogenet Evol 99:103–115. https://doi.org/10.1016/j.ympev.2016.02.013

Taylor SA, Larson EL (2019) Insights from genomes into the evolutionary importance and prevalence of hybridization in nature. Nat Ecol Evol 3:170–177. https://doi.org/10.1038/s41559-018-0777-y

Valtueña FJ, López J, Álvarez J, et al (2016) Scrophularia arguta, a widespread annual plant in the Canary Islands: a single recent colonization event or a more complex phylogeographic pattern? Ecol Evol 6:4258–4273. https://doi.org/10.1002/ece3.2109

840 Wada S, Kameda Y, Chiba S (2013) Long-term stasis and short-term divergence in the
841 phenotypes of microsnails on oceanic islands. Mol Ecol 22:4801–10.
842 https://doi.org/10.1111/mec.12427

843 Wares JP, Cunningham CW (2001) Phylogeography and historical ecology of the North Atlantic
844 intertidal. Evolution 55:2455–2469. https://doi.org/10.1111/j.0014-3820.2001.tb00760.x

845 Weber AA-T, Stöhr S, Chenuil A (2019) Species delimitation in the presence of strong
846 incomplete lineage sorting and hybridization. Mol Phylogenet Evol 131:240218.
847 https://doi.org/10.1101/240218

848 Weir BS, Cockerham CC (1984) Estimating F-statistics for the analysis of population structure.
849 Evolution (N Y) 38:1358–1370. https://doi.org/10.2307/2408641

850 Westheide W, Purschke G (1988) Organism processing. In: Higgins RP, Thiel H (eds)
851 Introduction to the study of meiofauna. Smithsonian Institution Press, Washington, pp 146–
852 160

853 Zanol J, Halanych KM, Struck TH, Fauchald K (2010) Phylogeny of the bristle worm family
854 Eunicidae (Eunicida, Annelida) and the phylogenetic utility of noncongruent 16S, COI and
855 18S in combined analyses. Mol Phylogenet Evol 55:660–676.
856 https://doi.org/10.1016/j.ympev.2009.12.024

857 Zuccarello GC, West JA, Kamiya M (2018) Non-monophyly of Bostrychia simpliciuscula
858 (Ceramiales, Rhodophyta): Multiple species with very similar morphologies, a revised
859 taxonomy of cryptic species. Phycol Res 66:100–107. https://doi.org/10.1111/pre.12207

860

861

862

Figure 1

Figure 1. Sampling locations across the Northern Atlantic.

A-B) North America, C) United Kingdom, France and Germany, and the Island of Sylt in Germany. The three species are displayed in different colours: orange (*Stygocapitella westheidei*), green (*S. josemariobrancoi*) and blue (*S. subterranea*). Sampling locations with multiple circles denote populations in sympatry. Species are delimited using the COI, 16S, 18S and ITS1 barcodes.

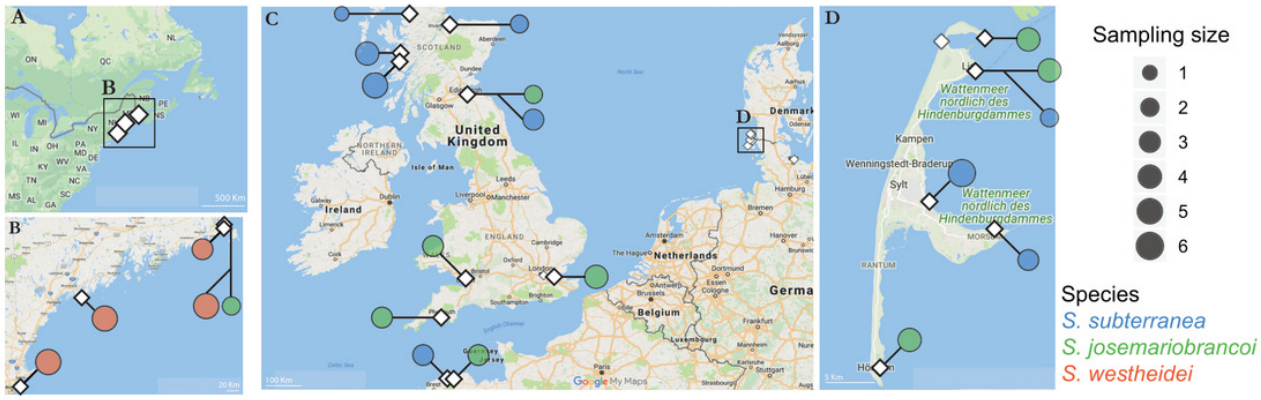
A
B
C
D
United Kingdom
Ireland
Netherlands
Belgium
Wattenmeer nördlich des Hindenburgdammes
Kampen
Wenningstedt-Braderup
Sylt
Sampling size
1
2
3
4
5
6
Species
S. subterranea
S. josemariobrancoi
S. westheidei

Figure 2

Figure 2. Phylogenetic reconstruction and Scanning Electron Microscopy images of *Stygocapitella*.

A) Maximum likelihood phylogeny of a concatenated, partitioned dataset (COI, 16S, 18S and ITS1), with scale provided on the bottom. Coloration follows species, with blue representing *Stygocapitella subterranea*, green representing *S. josemariobrancoi*, and orange *S. westheidei*. Bootstrap support for the branches representing species are provided on top of the branches. Every species is retrieved as monophyletic. B) Drawing of the *Stygocapitella westheidei, S. subterranea, S. josemariobrancoi* morphotype. For more information on the classification and distinction of the morphotypes see Cerca et. al (2020). C) Phylogenomic tree based on 4,737 RADseq loci. Bootstrap support is provided for the main branches. Coloration follows species with blue representing *Stygocapitella subterranea*, green representing *S. josemariobrancoi*, and orange *S. westheidei*. Three specimens, denoted by arrows, are identified as 'paraphyletic', including Bristol Channel 422 04 (identified as *S. josemariobrancoi*, nested within *S. subterranea*), Bristol Channel 422 05 (identified as *S. josemariobrancoi*, nested within *S. westheidei*) and St. Efflam 401 03 (identified as *S. josemariobrancoi*, nested sister to *S. subterranea*). The tree topology is coloured with shared pairwise data as estimated by BaCoCa. Allele 0 and allele 1 are displayed for all specimens. Specimen 222_01 is a technical replicate and is therefore represented twice. Shared pairwise data was calculated by integrating BaCoCa's information on pairwise missing data.

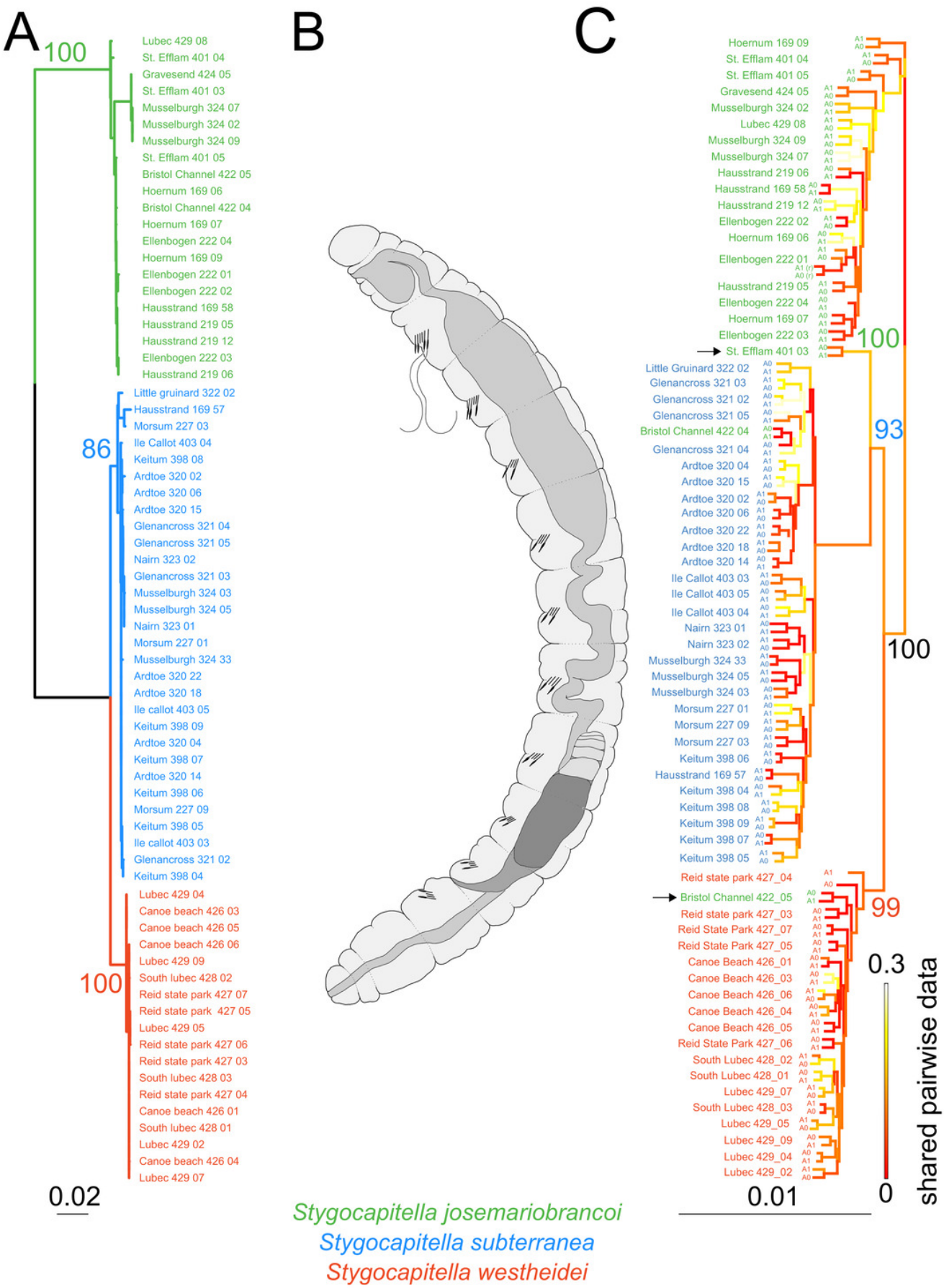
A
100
Lubec 429 08
St. Efflam 401 04
Gravesend 424 05
St. Efflam 401 03
Musselburgh 324 07
Musselburgh 324 02
Musselburgh 324 09
St. Efflam 401 05
Bristol Channel 422 05
Hoernum 169 06
Bristol Channel 422 04
Hoernum 169 07
Ellenbogen 222 04
Hoernum 169 09
Ellenbogen 222 01
Ellenbogen 222 02
Hausstrand 169 58
Hausstrand 219 05
Hausstrand 219 12
Ellenbogen 222 03
Hausstrand 219 06
86
Little gruinard 322 02
Hausstrand 169 57
Morsum 227 03
Ile Callot 403 04
Keitum 398 08
Ardtoe 320 02
Ardtoe 320 06
Ardtoe 320 15
Glenancross 321 04
Glenancross 321 05
Nairn 323 02
Glenancross 321 03
Musselburgh 324 03
Musselburgh 324 05
Nairn 323 01
Morsum 227 01
Musselburgh 324 33
Ardtoe 320 22
Ardtoe 320 18
Ile callot 403 05
Keitum 398 09
Ardtoe 320 04
Keitum 398 07
Ardtoe 320 14
Keitum 398 06
Morsum 227 09
Keitum 398 05
Ile callot 403 03
Glenancross 321 02
Keitum 398 04
100
Lubec 429 04
Canoe beach 426 03
Canoe beach 426 05
Canoe beach 426 06
Lubec 429 09
South lubec 428 02
Reid state park 427 07
Reid state park 427 05
Lubec 429 05
Reid state park 427 06
Reid state park 427 03
South lubec 428 03
Reid state park 427 04
Canoe beach 426 01
South lubec 428 01
Lubec 429 02
Canoe beach 426 04
Lubec 429 07
0.02
B
C
Hoernum 169 09
St. Efflam 401 04
St. Efflam 401 05
Gravesend 424 05
Musselburgh 324 02
Lubec 429 08
Musselburgh 324 09
Musselburgh 324 07
Hausstrand 219 06
Hausstrand 169 58
Hausstrand 219 12
Ellenbogen 222 02
Hoernum 169 06
Ellenbogen 222 01
Hausstrand 219 05
Ellenbogen 222 04
Hoernum 169 07
Ellenbogen 222 03
St. Efflam 401 03
100
Little Gruinard 322 02
Glenancross 321 03
Glenancross 321 02
Glenancross 321 05
Bristol Channel 422 04
Glenancross 321 04
Ardtoe 320 04
Ardtoe 320 15
Ardtoe 320 02
Ardtoe 320 06
Ardtoe 320 22
Ardtoe 320 18
Ardtoe 320 14
93
Ile Callot 403 03
Ile Callot 403 05
Ile Callot 403 04
Nairn 323 01
Nairn 323 02
Musselburgh 324 33
Musselburgh 324 05
Musselburgh 324 03
Morsum 227 01
Morsum 227 09
Morsum 227 03
Keitum 398 06
Hausstrand 169 57
Keitum 398 04
Keitum 398 08
Keitum 398 09
Keitum 398 07
Keitum 398 05
100
Reid state park 427_04
Bristol Channel 422_05
99
Reid state park 427_03
Reid State Park 427_07
Reid State Park 427_05
Canoe Beach 426_01
Canoe Beach 426_03
Canoe Beach 426_06
Canoe Beach 426_04
Canoe Beach 426_05
Reid State Park 427_06
South Lubec 428_02
South Lubec 428_01
Lubec 429_07
South Lubec 428_03
Lubec 429_05
Lubec 429_09
Lubec 429_04
Lubec 429_02
0.01
0.3
0
shared pairwise data
Stygocapitella josemariobrancoi
Stygocapitella subterranea
Stygocapitella westheidei

Figure 3

Phylogenetic network based on 4,737 RADseq loci.

Coloration follows species with blue representing *Stygocapitella subterranea*, green representing *S. josemariobrancoi*, and orange representing *S. westheidei*. Specimens with arrows represent specimens which were as paraphyletic in the phylogenomic tree (Fig. 2C). *S. josemariobrancoi* is clearly stretched, indicating a greater differentiation from the remaining two species. In congruence with the phylogenomic analysis, Bristol Channel 422 04 is nested within *S. subterranea.*

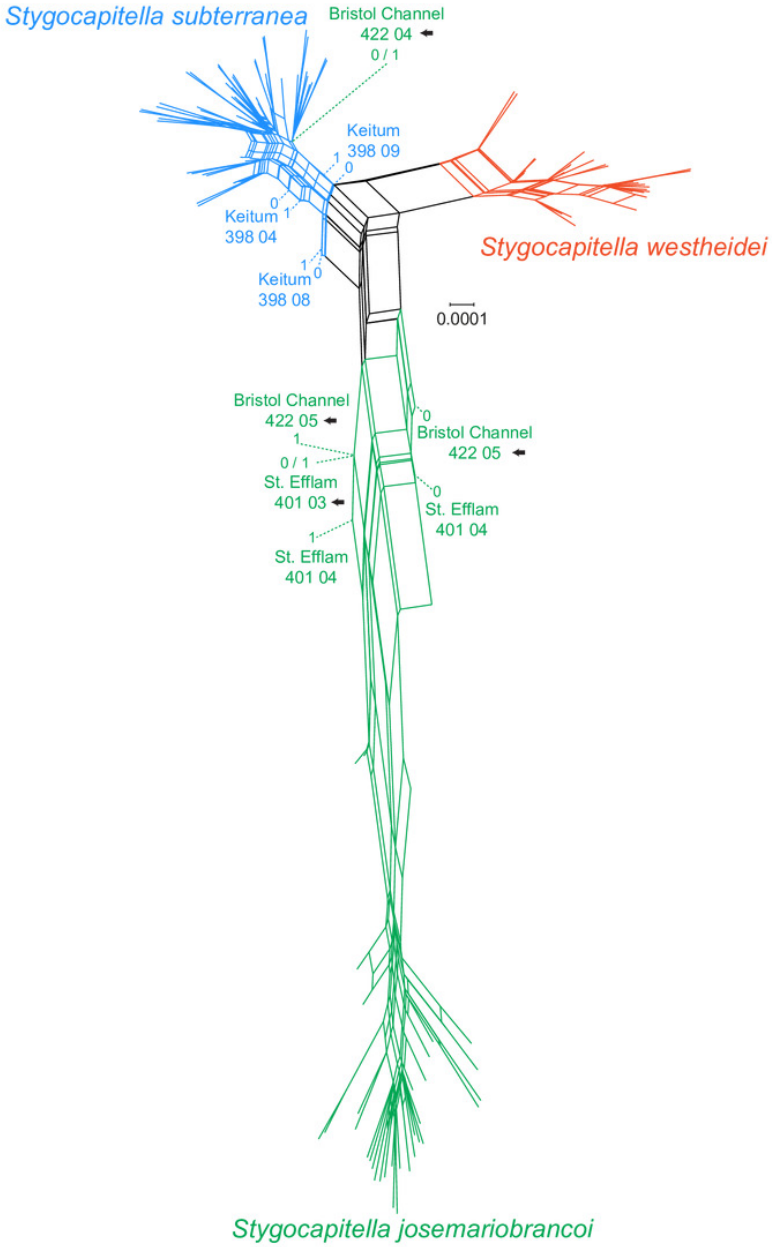
Stygocapitella subterranea
Bristol Channel
422 04
0 / 1
Keitum
398 09
1
0
0
1
Keitum
398 04
1
0
Keitum
398 08
Stygocapitella westheidei
0.0001
Bristol Channel
422 05
1
0 / 1
St. Efflam
401 03
1
St. Efflam
401 04
0
Bristol Channel
422 05
0
St. Efflam
401 04
Stygocapitella josemariobrancoi

Figure 4

Principal Component Analysis (A) and Multi-dimensional scaling (B) of 3,428 SNPs.

The percentage of explained variation is displayed with the axis for the PCA. Lineage (species) are given in different shapes, with colours represent populations. Specimens with ‘intermediate positions’ are highlighted both analyses, indicating potential shared generated variation between specimens.

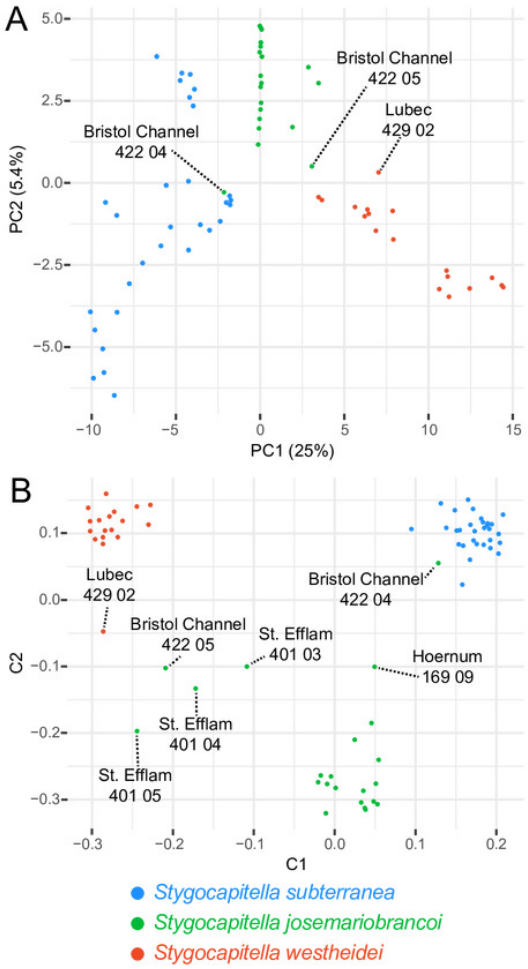
A
Bristol Channel 422 05
Lubec 429 02
Bristol Channel 422 04
PC2 (5.4%)
PC1 (25%)
B
Lubec 429 02
Bristol Channel 422 04
Bristol Channel 422 05
St. Efflam 401 03
Hoernum 169 09
St. Efflam 401 04
St. Efflam 401 05
C2
C1
Stygocapitella subterranea
Stygocapitella josemariobrancoi
Stygocapitella westheidei

Figure 5

ADMIXTURE analysis of 3,428 SNPs shows shared genetic variation.

Stygocapitella josemariobrancoi, *S. subterranea* and *S. westheidei* are plotted consecutively from left to right. Populations and specimen-ids are denoted at the bottom, with sympatric-populations in bold and italics. The cladogram follows the tree topology retrieved in Figure 2 A and 2 B.

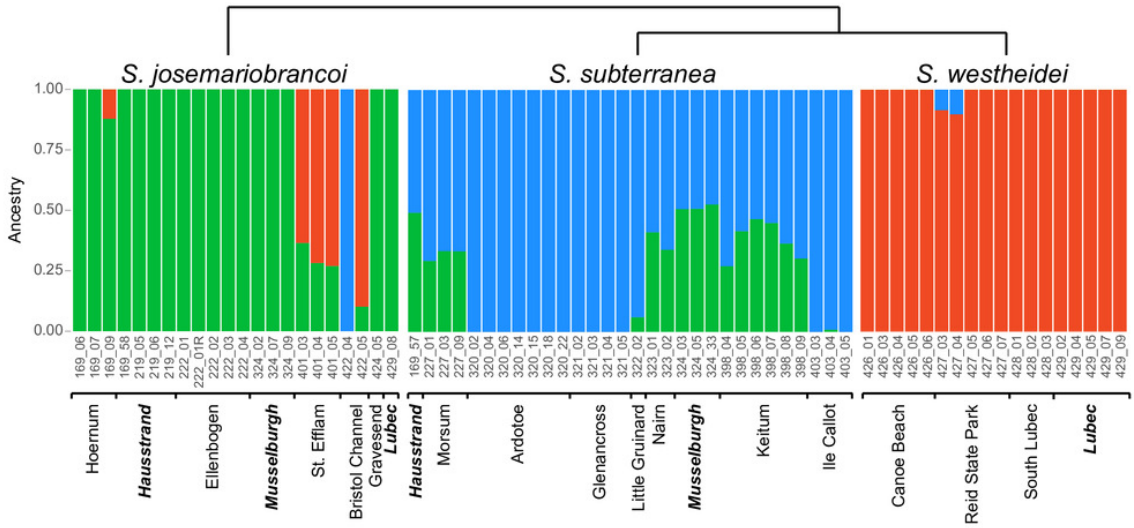
S. josemariobrancoi
S. subterranea
S. westheidei
Ancestry
1.00
0.75
0.50
0.25
0.00
169_06 169_07 169_09 169_58 219_05 219_06 219_12 222_01 222_01R 222_02 222_03 222_04 324_02 324_07 324_09 401_03 401_04 401_05 422_04 422_05 424_05 429_08
169_57 227_01 227_03 227_09 320_02 320_04 320_06 320_14 320_15 320_18 320_22 321_02 321_03 321_04 321_05 322_02 323_01 323_02 324_03 324_05 324_33 398_04 398_05 398_06 398_07 398_08 398_09 403_03 403_04 403_05
426_01 426_03 426_04 426_05 426_06 427_03 427_04 427_05 427_06 427_07 428_01 428_02 428_03 429_02 429_04 429_05 429_07 429_09
Hoernum
Hausstrand
Ellenbogen
Musselburgh
St. Effiam
Bristol Channel
Gravesend
Lubec
Hausstrand
Morsum
Ardotoe
Glenancross
Little Gruinard
Nairn
Musselburgh
Keitum
Ile Callot
Canoe Beach
Reid State Park
South Lubec
Lubec

Figure 6

Demographic scenarios considered.

The likelihood of different demographic scenarios is displayed on the Y axis. Based on the estimated phylogeny (Figure 2), we modelled scenarios for (from left to right): 1) gene flow only between S. westheidei and S. subterranea; 2) gene flow between S. josemariobrancoi and the lineage before the S. subterranea and S. westheidei split; 3) no gene flow at all; 4) gene flow between S. josemariobrancoi and S. subterranea, and between S. josemariobrancoi and the ancient lineage; 5) geneflow between lineages living in sympatry; 6) gene flow in every possible branch; 7) gene flow in sympatric, European linages; 8) gene flow between S. josemariobrancoi and S. westheidei; 9) gene flow between currently existing lineages.

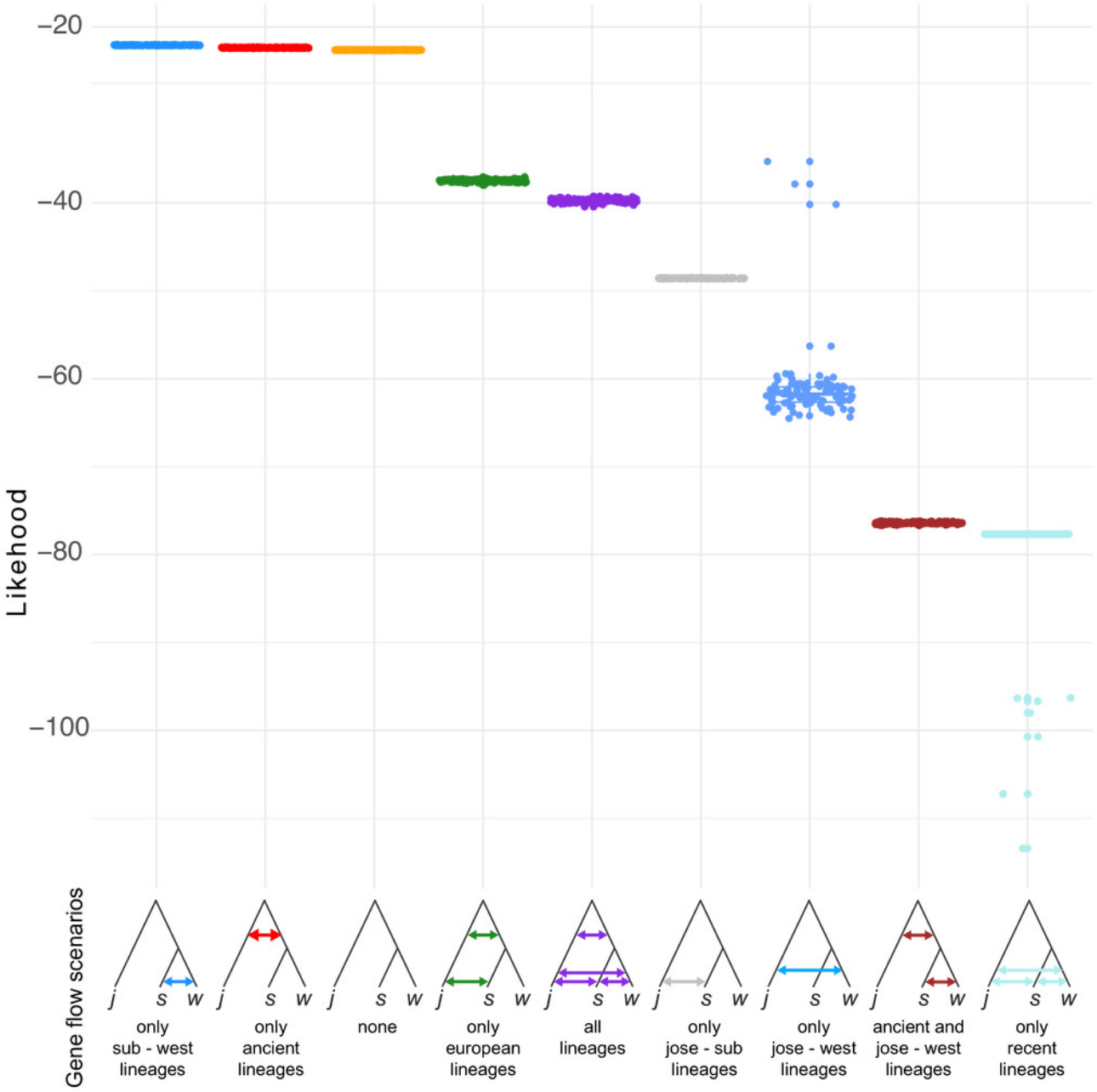
Likehood
−20
−40
−60
−80
−100
Gene flow scenarios
j s w
only sub - west lineages
only ancient lineages
none
only european lineages
all lineages
only jose - sub lineages
only jose - west lineages
ancient and jose - west lineages
only recent lineages

Table 1(on next page)

ƒ3 statistics testing for hybridization between lineages.

Each row represents a scenario where two species are the source for admixture, and the third species is the target of hybridization. A ƒ3 statistic, the standard error (SE) and a Z-score value calculated with jackknife is provided for each scenario based.

Table 1 *f*3 statistics testing for hybridization between lineages. Each row represents a scenario where two species are the source for admixture, and the third species is the target of hybridization. A *f*3 statistic, the standard error (SE) and a Z-score value calculated with jackknife is provided for each scenario based.

Source 1	Source 2	Target	*f*3	SE	Z
S. subterranea	*S. josemariobrancoi*	*S. westheidei*	0.91	0.08	11.424
S. josemariobrancoi	*S. westheidei*	*S. subterranea*	1.09	0.24	4.575
S. westheidei	*S. subterranea*	*S. josemariobrancoi*	0.25	0.10	2.605

Table 2(on next page)

Weir-Cockherham Fst-estimate

Estimates are provided in the lower part of the table, and the number of individuals included in the pairwise estimation is provided in the upper part of the table.

Table 2 Weir-Cockherham Fst-estimate is provided in the lower part of the table, and the number of individuals included in the pairwise estimation is provided in the upper part of the table.

Species	*S. subterranea*	*S. josemariobrancoi*	*S. westheidei*
S. subterranea	-	52	48
S. josemariobrancoi	0.530	-	40
S. westheidei	0.664	0.492	-

Table 3(on next page)

Summary statistics for the various analysed populations

For each site we provide the number of specimens and chromossomes, number of loci considered, S (Waterson's estimate), the averaged π, and the averaged Tajima's D. Analysed populations include those with >5 chromossomes, with the exception of Plymouth which had no samples with no missing data.

Table 3 Summary statistics for the various analysed populations. For each site we provide the number of specimens and chromossomes, number of loci considered, S (Waterson's estimate), the averaged π, and the averaged Tajima's D. Analysed populations include those with >5 chromossomes, with the exception of Plymouth which had no samples with no missing data.

Species	Site	Number of specimens (chromossomes)	Number of loci analyzed (without missing data)	S (Waterson's estimate)	Averaged π	Averaged Tajima's D
Stygocapitella subterranea	Ardtoe	7 (14)	122	2.1066	0.0020	-0.1843
	Glenancross	4 (8)	658	2.1763	0.0029	0.1123
	Hausstrand	1 (not analyzed)	-		-	
	Ile Callot	3 (6)	1301	2.3912	0.0037	0.1958
	Keitum	6 (12)	40	2.525	0.0030	-0.1858
	Little Gruinard	1 (not analyzed)	-	-	-	-
	Morsum	3 (6)	1923	2.1482	0.0032	0.1326
	Musselburgh	3 (6)	1166	2.1329	0.0033	0.1571
	Nairn	2 (not analyzed)	-	-	-	-
Stygocapitella josemariobrancoi	Bristol Channel	2 (not analyzed)	-	-	-	-
	Ellenbogen	4 (8)	403	1.6377	0.0024	-0.1993
	Gravesend	2 (not analyzed)	-	-	-	-
	Hausstrand	4 (8)	154	2.5519	0.0038	-0.3862
	Hoernum	3 (6)	261	2.6858	0.0046	-0.0281
	Lubec	1 (not analyzed)	-	-	-	-
	Plymouth	0 (not analyzed)	-	-	-	-
	Musselburgh	3 (6)	414	2.5918	0.0045	-0.0356
	Saint Efflam	3 (6)	572	3.3969	0.0059	0.1702
Stygocapitella westheidei	Canoe Beach	5 (10)	577	1.8128	0.0021	-0.3654
	Lubec	5(10)	89	2.1461	0.0029	-0.1044
	Reid State Park	5 (10)	519	2.3468	0.0024	-0.5266
	South Lubec	3 (6)	524	2.0115	0.0034	0.1723